ACS APPLIED MATERIALS & INTERFACES

Research Article

www.acsami.org

# Synergistic Effects of a Multifunctional Graphene Based Interlayer on Electrochemical Behavior and Structural Stability

Young-Woo Lee,[†] Geon-Hyoung An,[‡] Byung-Sung Kim,[†] John Hong,[†] Sangyeon Pak,[†] Eun-Hwan Lee,[‡] Yuljae Cho,[†] Juwon Lee,[†] Paul Giraud,[†] Seung Nam Cha,[†] Hyo-Jin Ahn,*[,‡] Jung Inn Sohn,*[,†] and Jong Min Kim[†]

[†]Department of Engineering Science, University of Oxford, Oxford OX1 3PJ, U.K.

[‡]Department of Materials Science and Engineering, Seoul National University of Science and Technology, Seoul 139-743, Republic of Korea

Supporting Information

**ABSTRACT:** The ability to rationally design and manipulate the interfacial structure in lithium ion batteries (LIBs) is of utmost technological importance for achieving desired performance requirements as it provides synergistic effects to the electrochemical properties and cycling stability of electrode materials. However, despite considerable efforts and progress made in recent years through the interface engineering based on active electrode materials, relatively little attention has been devoted to address the physical aspects of the interface and interfacial layer between the anode materials layer and the current collector. Here, we propose and successfully grow unique graphene directly on a Cu current collector as an ideal interfacial layer using the modified chemical vapor deposition (CVD). The anode with an engineered graphene interlayer exhibits remarkably improved electrochemical performances, such as large reversible specific capacity (921.4 mAh $g^{-1}$ at current density of 200 mA $g^{-1}$), excellent Coulombic efficiency (close to approximately 96%), and superior cycling capacity retention and rate properties compared to the bare Cu. These excellent electrochemical features are discussed in terms of multiple beneficial effects of graphene on interfacial stability and adhesion between the anode and the collector, oxidation or corrosion resistance of the graphene grown Cu current collector, and electrical contact conductance during the charge/discharge process.

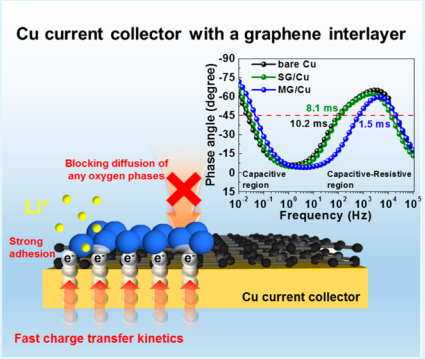


**KEYWORDS:** *interface engineering, graphene, electrochemical behavior, 2D interlayer, structural stability, energy storage*

## INTRODUCTION

Interface engineering has drawn considerable research interest for both fundamental science and cutting-edge technology because the diverse and unique properties of devices with geometric architectures of multistacked functional layers are crucially dependent on the physical and chemical states of homogeneous/heterogeneous interfaces between each functional layer, which can play an important role in determining their electronic, optoelectronic, and electrochemical behaviors as well as structural stability and quality.[1−5] Thus, interface engineering through interface modification and functionalization methods has been proven to be a very effective and important step toward improving the device performance of semiconductor and solid-state energy devices. In particular, much attention has been focused recently on the development of new functional interfacial materials.[6,7]

In this regard, graphene with the inherent 2-dimensional nature of a crystal structure has attracted tremendous attention as an atomically ultrathin interfacial layer because of its unique and outstanding electrical, optical, chemical, and mechanical properties, which can allow for atomic-scale engineering of interlayers to achieve uniform interfacial coverage, to improve electrical interface contact or charge carrier transport efficiency, to manipulate energy level alignment, to enhance interfacial adhesion, and to maintain mechanical and chemical stability.[8,9] These properties of graphene make it a promising material for the use in a wide range of growing applications including various electrical and optoelectronic devices as well as energy conversion and storage devices without need for binders, additives, and current collectors.[10,11]

On the basis of diverse interface engineering techniques, so far, the LIBs regarded as promising energy storage devices have been widely studied to fulfill high energy and power densities, long cyclic stability, and high rate capability by employing various strategies, such as the engineered nanostructure with controlled shape and morphology as well as size, the controlled modification of pore structures with large surface area, and surface modification and functionalization.[12,13] Among such diverse interface engineering techniques researched to date, the surface modification has intensively emerged in recent as a

Received: March 31, 2016
Accepted: June 20, 2016
Published: June 20, 2016




DOI: 10.1021/acsami.6b03866
ACS Appl. Mater. Interfaces 2016, 8, 17651−17658

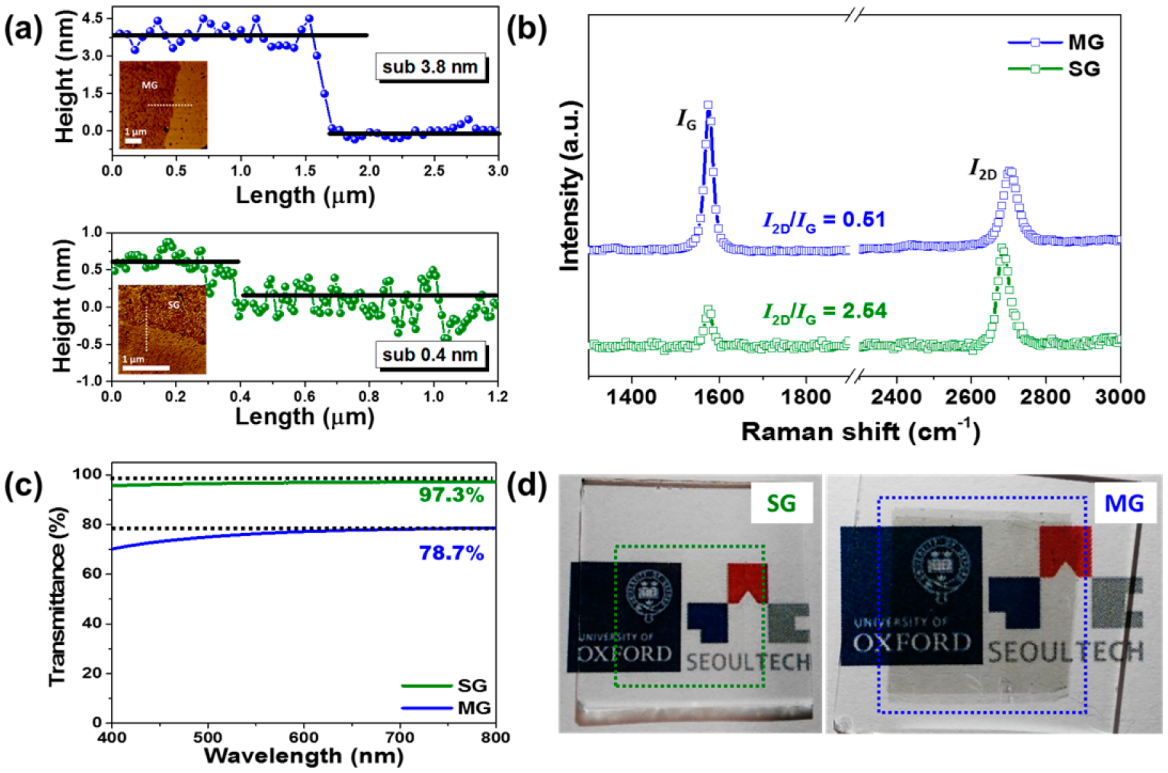


**Figure 1.** (a) The corresponding line scans across the edge of the multi- and single-layered graphene transferred on a $SiO_2$ substrate [the insets indicate the high-resolution AFM image of multi- and single-layered graphene]. (b) Raman spectrum of the multi- and single-layered graphene films. (c) Optical transmittance and (d) photographic transparency of graphene films with multilayer and single layer.

highly promising and attractive approach to enhance electrical conductivity, structural stability, ion and electron transport, cyclability, and reliability more effectively.[14−17] However, most studies of the interface engineering associated with surface modification continue to mainly focus on the interfaces between the active electrode material and the electrolyte in order to improve the electrochemical performance of electrode materials. Contrastively, interfacial effects occurring between the active electrode and the current collector have received relatively little attention and consequently are not well understood, although the engineering and optimization of such interface states are very important to improve and retain good electrical contact and chemical and structural stability, which could be critical factors determining the performance and lifetime of LIBs.

To this end, herein we propose to use high-quality, large-area CVD graphene grown directly on Cu current collectors as an ideal and efficient interlayer between the active material and the metallic current collector for LIBs from the viewpoint of the following potential synergistic benefits: (1) the chemically stable graphene can behave as an efficient diffusion barrier to resist the degradation by effectively preventing the formation of the oxidized layer on the metallic current collector surface through oxygen diffusion provided by electrolyte decomposition and/or byproduction during Li ion intercalation reactions; (2) the outstanding electrical conductivity of graphene can form high-quality contact with low interface resistance, thus facilitating the fast charge transfer process; (3) the excellent structural flexibility and mechanical robustness of graphene might enhance the physical interface adhesion, thereby minimizing the issues associated with the progressive loss of contact area induced by stress built up at the interface during the long-term cyclic reaction. By designing and developing unique interfacial graphene layers, we demonstrate that the engineered graphene based interfacial layer on the current collector can remarkably improve electrochemical properties, such as specific reversible capacity, capacity retention, rate performance, and charge transfer ability and Li ion diffusion rates, compared to the pure Cu current collector.

## EXPERIMENTAL SECTION

**Synthesis of the Graphene Interlayer on the Current Collector.** The 250 $\mu$m thick Cu foil was first cleaned with a 1 M HCl solution, followed by washing the foil with acetone, ethanol, and DI water. The Cu foil was placed in a CVD furnace, and the furnace was evacuated down to a pressure of 2 mTorr. The temperature of the furnace was, then, heated to 1000 °C at a rate of 25 °C/min with $H_2$ gas flow of 5 sccm. After annealing the foil at 1000 °C for 20 min, the synthesis of graphene was initiated with flowing methane gas of 20 sccm (single layer) or 50 sccm (multilayer) for 40 min while maintaining the same temperature. After the completion of the growth, the furnace was rapidly cooled (single layer) or slowly cooled (multilayer) to room temperature. To estimate thickness and transmittance of as-prepared graphene samples, the graphene was transferred using a copper etchant (0.1 M ammonium persulfate) to a $SiO_2$ and glass substrate.

**Chemical and Structural Characterization.** The morphology and the thickness uniformity of graphene were observed by AFM (Veeco dimension 3100). The defect and quality of graphene were investigated by Raman spectroscopy (Nanofinder 30) with a 488 nm wavelength diode-pumped solid-stage laser. The optical transmission spectra of graphene were obtained by UV−vis−NIR spectrophotometry (Varian Cary 5000). The chemical bonding states of the graphene interlayer were examined by XPS (ESCALAB250) equipped with an Al K$\alpha$ X-ray source. The C 1s electron binding energy was referenced at 285.0 eV, and a nonlinear least-squares curve-fitting program was employed with a Gaussian−Lorentzian production


DOI: 10.1021/acsami.6b03866
ACS Appl. Mater. Interfaces 2016, 8, 17651−17658

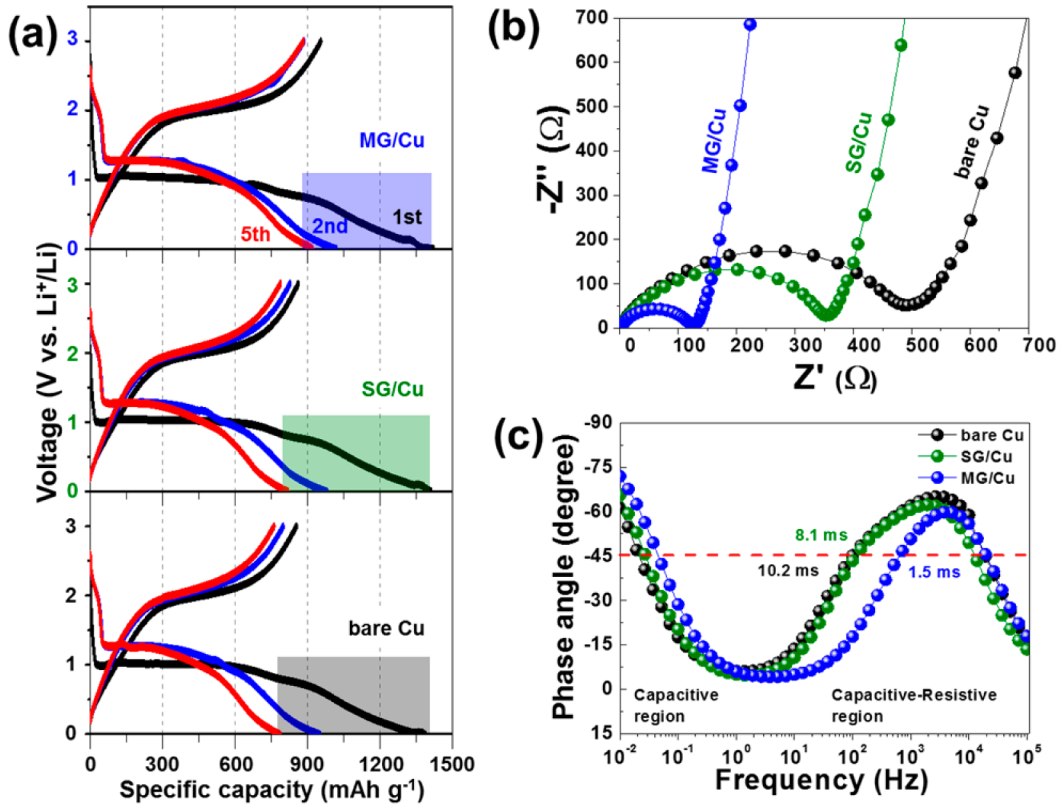


**Figure 2.** (a) Galvanostatic discharge−charge curves of $Co_3O_4$ based anodes on MG/Cu, SG/Cu, and bare Cu for the first, second, and fifth cycles at a current density of 200 mA $g^{-1}$ in the voltage range of 0.0−3.0 V. (b) Nyquist plots of the MG/Cu, SG/Cu, and bare Cu in a frequency range of 100 kHz to 10 mHz. (c) Bode plots of MG/Cu, SG/Cu, and bare Cu, fitted using the simplified equivalent circuit.

function. Also, the film structures of as-prepared electrodes were characterized using SEM (Hitachi S-4700).

**Electrochemical Measurement.** The electrochemical performance of electrodes was performed using a coin-type half cell (CR2032) with $Co_3O_4$ on MG/Cu, SG/Cu, and bare Cu as a current collector. The homogenized slurry made of 70 wt % $Co_3O_4$ (Sigma-Aldrich) as an active material, 20 wt % poly(vinylidene difluoride) (Alfa Aesar) as a binder, and 10 wt % Ketjen black (Mitsubishi Chemical) as a conducting material in *N*-methyl-2-pyrrolidinone (Sigma-Aldrich) was coated on the as-prepared current collectors and then dried at 100 °C for 12 h. The coin-type half cells were fabricated in a glovebox filled with argon gas. The charge/discharge performance was evaluated using a WMPG 3000 battery cycler system (WonATech Corp., Korea) in the potential window of 0.0−3.0 V (vs $Li/Li^+$) at room temperature. The cycling test was performed up to 100 cycles at a current density of 200 mA $g^{-1}$. The high-rate capability was investigated at current densities of 200, 500, 1000, and 1500 mA $g^{-1}$. The EIS measurements were characterized in a frequency range of 100 kHz to 10 mHz at an ac signal of 5 mV.

## RESULTS AND DISCUSSION

To form a geometrically attractive interfacial structure between the active material and the metallic current collector, allowing the favorable electrochemical behavior of Li ions, a modified CVD method has been employed. We successfully synthesized single- and multilayered graphene on Cu foil (denoted as "SG/Cu" and "MG/Cu", respectively) with large scale area ($6_{height}$ × $14_{width}$ cm, as shown in Figure S1) under different flow rates of methane gas (see more detailed Experimental Section) for investigating in detail interfacial effects. Figure 1a exhibits typical tapping-mode atomic force microscope (AFM) images of SG and MG transferred onto a $SiO_2$ substrate, confirming the formation of layered graphene structures. A line scan across the edge of SG/Cu reveals a distinct step of approximately 0.4 nm, which is in good agreement with the thickness (0.34 nm) of the single graphene layer.[18−20] Contrastively, the topographic height profile of MG/Cu exhibits the edge of thin graphene layers with a step of ∼3.8 nm, corresponding to the multilayered graphene with approximately 10 layers. For further confirmation of the number and the uniformity of graphene layers, we performed Raman and UV−vis spectroscopy analyses. Figure 1b shows that all Raman spectra exhibit two dominant peaks at around 1576 and 2686 $cm^{-1}$, corresponding to the G and 2D mode, respectively, which are the typical features of graphene. Moreover, the layer number of graphene was also identified by the intensity ratio of the 2D to G peaks ($I_{2D}/I_G$), which have been known to be especially sensitive to the number of graphene layers.[21,22] That is, for SG/Cu the $I_{2D}/I_G$ intensity ratio of 2.54 indicates that the formed graphene film has single layer with high quality, whereas the intensity ratio of MG/Cu is 0.51, showing a typical signature of multilayered graphene. In addition, it can be seen in Figure 1c that the optical transmittance of SG (97.3%) and MG films (78.7%), which is determined by the number of layers, clearly indicating the formation of single-layer and multilayer (∼10 layers) graphene films.[23−25] This is consistent with AFM results and previous reports. Moreover, Figure 1d shows the photograph of high transparency of SG and MG on a glass substrate. The symbols behind can be clearly seen through the graphene layer without distorting the image, which is consistent with optical transmittance results. To determine the surface chemical states of as-prepared graphene interlayers, we performed X-ray photoelectron spectroscopy (XPS) measurements. We clearly observed that SG/Cu and MG/Cu samples


DOI: 10.1021/acsami.6b03866
ACS Appl. Mater. Interfaces 2016, 8, 17651−17658

exhibit the typical carbon characteristic in the C 1s spectra, implying the successful formation of graphene layers (Figure S2). On the basis of the structural and chemical analyses of as-prepared graphene, we believe that the SG/Cu and MG/Cu have a well-defined layered, large-scale structure with high quality. Accordingly, it can be expected that the graphene grown directly on current collectors as an interfacial layer will significantly improve the electrochemical and structural properties during the charge/discharge process because of its uniform coverage on Cu foil, high electrical conductivity, and strong interfacial adhesion.

The ability to engineer the interface between the active material and the current collector, significantly affecting chemical and physical interfacial properties, would play an important role in improving the Li ion behavior properties. In order to investigate such interfacial effects on characteristics of LIBs, we performed the electrochemical characterization of a half coin cell using commercial $Co_3O_4$ anode materials as one of the representative high performance metal oxide anode materials, which still experiences obvious capacity fading typically resulting from relatively high interfacial contact resistance and unnecessary interfacial reactions as well as progressive loss of contact area on current collectors during cycling. Figure 2a shows the galvanostatic discharge−charge curves of $Co_3O_4$ based anodes on bare Cu, SG/Cu, and MG/Cu at a current density of 200 mA $g^{-1}$ in the voltage window of 0.0−3.0 V. During the first discharge process, we clearly observed that all electrodes exhibit a long potential plateau around at 1.0 V associated with the Li ion intercalation, that is, the formation of metallic Co and amorphous $Li_2O$ phases through the reduction reaction of $Co_3O_4$, followed by a gradual slope to the cutoff potential of 0.0 V, which is ascribed to the formation of a solid electrolyte interphase (SEI) layer by electrolyte decomposition.[26−29] In addition, it was observed that regardless of the presence of graphene interlayers, the specific discharge capacity of all samples is found to be very similar values of approximately 1400 mAh $g^{-1}$ with small variations in the first cycle, as summarized in Table S1. However, noticeably, it was observed that the $Co_3O_4$ anode on MG/Cu exhibits not only the significantly improved reversible specific discharge capacity of 921.4 mAh $g^{-1}$ compared to that anode on bare Cu (785.6 mAh $g^{-1}$) after the fifth cycle but also superior reversible Li ion behavior and the excellent Coulombic efficiency close to about 96% (Figure S3a). This enhanced capacity retention of the $Co_3O_4$ anode on MG/Cu with high specific capacity during the initial cycles might be attributed to the well-engineered graphene interlayer, which can not only influence electrochemical behavior properties but also contribute to the total capacity through Li ion intercalation into the multilayer graphene during the charge/discharge process. Moreover, in contrast to the MG/Cu, for the SG/Cu sample, a very slightly improvement in the capacity (818.9 mAh $g^{-1}$) was observed. These results indicate that the electrochemical characteristic of the $Co_3O_4$ anode is strongly dependent on the graphene interfacial layer.[30,31]

Moreover, in order to understand the electrochemical kinetic behavior of electrodes associated with the graphene interlayer, the electrochemical impedance spectroscopy (EIS) measurements as a powerful tool to investigate the charge transfer process were performed in a frequency range of 100 kHz to 10 mHz, as shown in Figure 2b. It can be seen distinctly that the charge transfer impedance ($R_{ct}$) of the MG/Cu (122.9 Ω) is much smaller than that of the SG/Cu (360.6 Ω) and bare Cu (503.7 Ω), implying that the presence of graphene interlayers improves the electrical contact and hence resulting in the enhanced charge transfer ability. To further evaluate the Li ion diffusion dynamics, the frequency dependence phase angle plots (Bode plots) were obtained and fitted using the simplified equivalent circuit, as shown in Figure 2c and summarized in Table S2. Here note that in general the low-frequency region, corresponding to the capacitive behavior, is associated with the Li ions diffusion and intercalation and that a phase angle approaching −90° indicates the ideal capacitive nature.[7,32−34] Thus, as expected, we observed that the MG/Cu exhibits a relatively higher phase angle compared to that of the SG/Cu and bare Cu, meaning superior capacitive feature. Furthermore, at the medium frequency range related to a capacitive-resistive transition region, the phase angle includes contributions from charge transfer effects at the interface.[35,36] We clearly observed the phase angle of the MG/Cu sample shows the relatively lower peak intensity and peak shift toward high frequency, indicating the low charge transfer impedance and the excellent ac response to the devices compared to the SG/Cu and bare Cu samples. Additionally, the relaxation time constant ($\tau_0$) is calculated with the equation $\tau_0 = 1/f_0$ in the interfacial charge transfer frequency region (10−$10^4$ Hz). The $\tau_0$ of the MG/Cu (1.5 ms) is shorter than that of the SG/Cu (8.1 ms) and bare Cu (10.2 ms). Such a rapid response property is attributed to the fast charge transport rate properties due to the presence of a graphene interfacial layer. Moreover, to further demonstrate effects of the engineered graphene interfacial layer on the electrochemical performance of LIBs, we employed $SnO_2$ as another representative metal oxide material. Similar to the $Co_3O_4$ based anode on MG/Cu, the $SnO_2$ based MG/Cu exhibited excellent Li ion behavior properties, such as the high discharge capacity, low charge transfer impedance, fast relaxation time constant, and enhanced initial electrochemical stability compared to the $SnO_2$ anode on bare Cu as shown in Figure S4. These findings suggest that the electrochemical performance of LIBs can be significantly enhanced by the graphene interlayer with superior electrical and mechanical contact properties as well as chemical stability, improving the charge transfer ability and Li ion diffusion rate.

To investigate in detail how the graphene interfacial layer affects electrochemical behavior and stability, we conducted long-term and intercalation-rate related electrochemical measurements together with impedance, chemical, and structural analysis techniques to analyze the interfacial features and structural stability. Noticeable, as shown in Figure S3a, the MG/Cu exhibited not only much better reversible capacity of 709 mAh $g^{-1}$ after 20 cycles at 200 mA $g^{-1}$ but also approximately 7.04 times higher reversible capacity and superior capacity retention after 100 cycles in comparison with the bare Cu. Furthermore, when the charge/discharge rate was increased stepwise from 200 to 1500 mA $g^{-1}$, the MG/Cu showed excellent rate capabilities (190 mAh $g^{-1}$ at 1500 mA $g^{-1}$), whereas both of the SG/Cu and bare Cu exhibited a rapid drop of initial capacity during 10 cycles and then rapidly decayed in the capacity with increasing rates, as shown in Figure S3b. Note that the rapid capacity fading and rate capabilities of bare Cu samples we observed are quite similar to the tendency of previous results for metal oxide anode materials.[37,38] Thus, these results imply that the cycling and rate behavior properties of anode could be significantly improved by simply modifying interfacial states between the active material and the Cu collector, which is thought to be a


DOI: 10.1021/acsami.6b03866
ACS Appl. Mater. Interfaces 2016, 8, 17651−17658

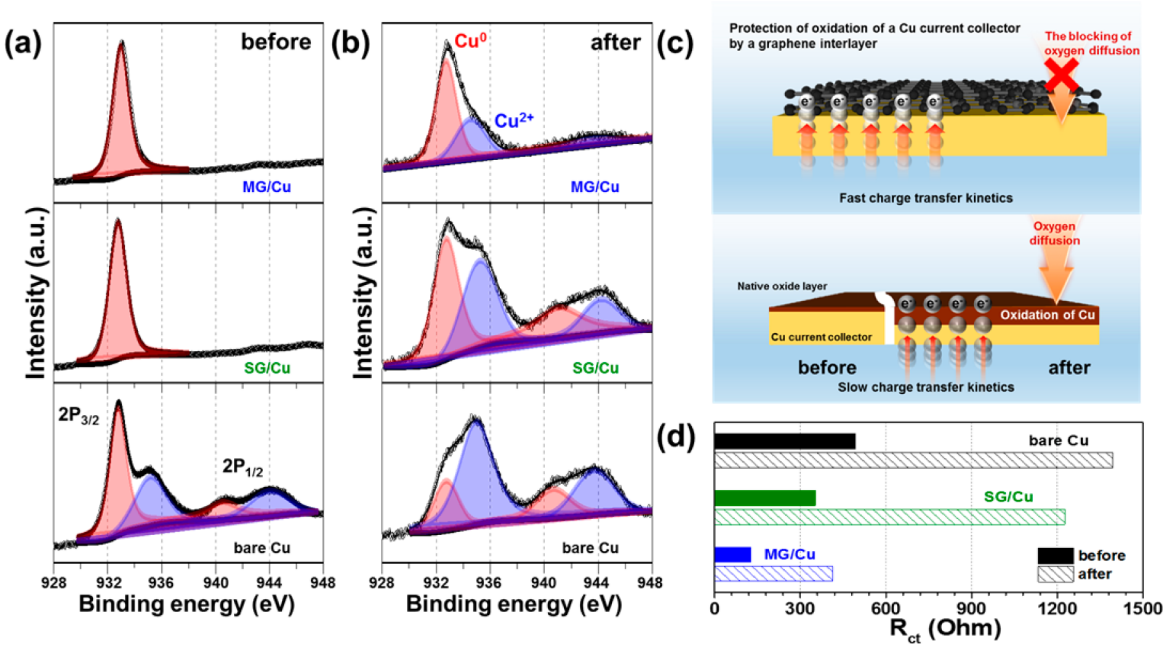


**Figure 3.** Cu 2p XPS spectra of MG/Cu, SG/Cu, and bare Cu at the interface (a) before and (b) after 100 cycling tests at a current density of 200 mA $g^{-1}$. (c) Schematic illustration for synergistic effects of a graphene interfacial layer between the active material and the current collector on structural stability and electrochemical reaction behavior during the charge/discharge process in comparison with bare Cu. (d) Histogram of changes in $R_{ct}$ of the MG/Cu, SG/Cu, and bare Cu samples before and after cycling tests.

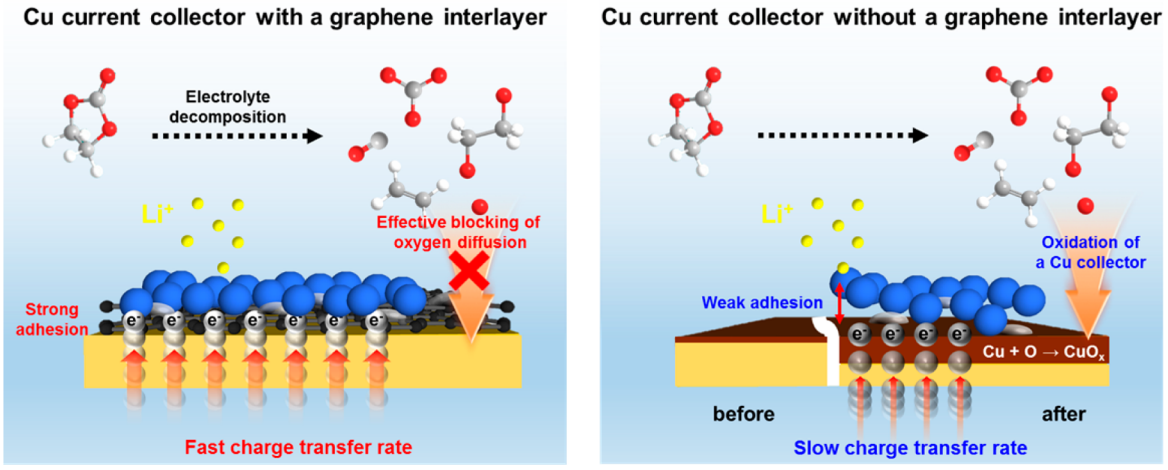


**Figure 4.** Schematic illustration showing the electrochemical and structural aspects of interfacial phenomena in LIB electrodes with and without a graphene interlayer.

critical consideration for optimizing electrochemical performance.

In order to further verify a detailed internal reaction at the interface during the charge/discharge process, we investigated phase changes in the evolution of interfacial structures on the Cu current collector by XPS before and after the long-term cycling test. Figure 3a shows the Cu 2p XPS spectra of the MG/Cu, SG/Cu, and bare Cu before the cycling test. We clearly observed that both the MG/Cu and SG/Cu samples exhibit only Cu $2p_{3/2}$ peaks at ~932.7 eV corresponding to the metallic Cu phases.[39,40] In contrast, for the bare Cu we observed an additional peak with binding energies of ~935.1 eV related to an oxidized Cu phase, which is attributed to the native oxide layer.[33] This finding suggests that the graphene interfacial layer can serve as a diffusion barrier, preventing the oxidization reaction of Cu. As expected, after 100 cycling tests the increase in the oxidized Cu phase of MG/Cu is relatively immaterial compared to the bare Cu and SG/Cu, showing the significant increase in the intensity of oxidized phases as a result of oxidation reactions of the Cu current collector through the byproducts generated from electrolyte decomposition during the charge/discharge reactions (Figure 3b). These phenomena were further confirmed by EIS measurements as shown in Figure 3d. We found that the MG/Cu exhibited less $R_{ct}$ change, which steadily maintains excellent electrical contact properties, after long-term cycling tests, while the $R_{ct}$ value of the other electrodes increases much more rapidly. Therefore, a comparison of the XPS and EIS results indicates that multilayered graphene is suitable to be used as an interfacial layer between the active material and the current collector in


DOI: 10.1021/acsami.6b03866
ACS Appl. Mater. Interfaces 2016, 8, 17651−17658

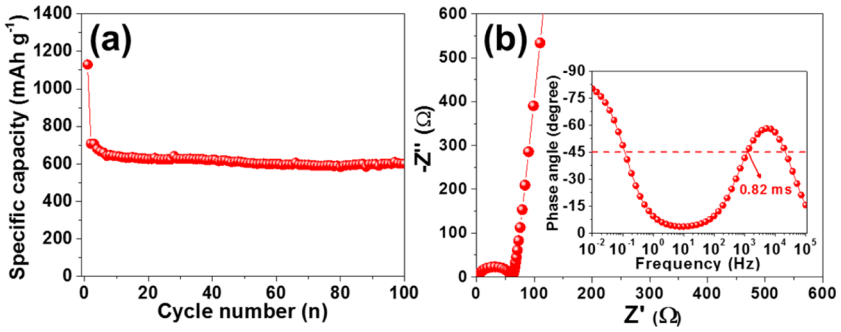


**Figure 5.** (a) Cycling performance of G+MG/Cu at a current density of 200 mA $g^{-1}$ up to 100 cycles in the voltage range of 0.0−3.0 V. (b) Nyquist plots of the G+MG/Cu in a frequency range of 100 kHz to 10 mHz. The inset indicates the Bode plots of the G+MG/Cu.

LIBs in order to effectively inhibit the oxidation of the Cu, hence retaining the low contact resistance as well as the high charge transfer rate, as illustrated in Figure 3c. In other words, the graphene interlayer with the suitable thickness and uniform coverage directly grown on the Cu collector can have strong resistance against interfacial reactions, substantially resulting in the battery performance deterioration due to the poor interfacial properties. To further demonstrate the structural integrity at the interface, we performed cross-sectional scanning electron microscopy (SEM) observations with all electrodes before and after the long-term cycling charge/discharge test, as shown in Figure S5. Interestingly, it was clearly observed that the presence of a graphene interfacial layer can lead to surprisingly improved adhesion of active materials to the Cu collector. However, the current collector without a graphene interlayer tends to show the weak interfacial adhesion, consequently causing the severe loss of electrical contact with active materials after cycling.

Here, we propose that an engineered interfacial layer has synergistic effects on the remarkable electrochemical performance and stability of LIB anodes we observed, as schematically illustrated in Figure 4: (1) The unique graphene interlayer with excellent electrical conductivity improves the charge transfer ability because of the low contact resistance. (2) The graphene with unique geometry and chemical stability effectively prevents the oxidation or corrosion reaction of a Cu current collector, which could be caused by the decomposition of electrolyte during charge/discharge reactions. (3) The directly grown graphene on the Cu collector possesses notable adhesive properties for firmly securing the interfacial adhesion strength between the active material and the current collector during the cycling. Consequently, by fully utilizing graphene's unique electrical, mechanical, structural, and chemical features, we remarkably enhance the cycling stability and performance of LIB anodes.

It should be also noted that metal oxide active materials exhibit substantially inferior capacity retention caused by large volume changes during the charge/discharge reaction. Thus, we believe that although the graphene-based interfacial engineering leads to a considerable enhancement in the electrochemical performance of anodes, the relatively low capacity is attributed to the structural degradation and instability caused mainly by the large volume change of commercial $Co_3O_4$ active materials we employed in this study, as shown in Figure S3a. In order to further optimize and demonstrate overall cell performance, we progressed additional interface engineering among active materials by mixing with multilayered graphene nanosheets (20 wt % vs weight of total active materials) on the MG/Cu electrode (G+MG/Cu). Figure 5a shows the cycling performance of the G+MG/Cu at a current density of 200 mA $g^{-1}$ in the voltage window of 0.0−3.0 V. Notably, the G+MG/Cu exhibited the higher initial reversible capacity of 708 mAh $g^{-1}$ in the second discharge reaction, which is comparatively close to the theoretical specific capacity of mixed G-$Co_3O_4$ (786.4 mAh $g^{-1}$) calculated on the basis of the weight ratio of each component (Figure S6a). More importantly, the G+MG/Cu sustained the high reversible capacity of 601 mAh $g^{-1}$ after 100 cycles. Furthermore, when current densities were increased from 200 (low-rate cycles) to 1500 mA $g^{-1}$ (high-rate cycles) in Figure S6b, the G+MG/Cu exhibited the significantly improved rate performance with capacity retention of 72.1% and high specific capacity of 505 mAh $g^{-1}$ at 1500 mA $g^{-1}$. Figure 5b shows Nyquist and Bode plots, indicating that the G+MG/Cu anode showed the improved charge transfer and fast Li ion diffusion properties due to the existence of graphene nanosheets among active materials, which could contribute to enhance electrical conductivity and as well as to prevent structural volume expansion acting as a physical buffer layer. Thus, as expected, it is believed that the remarkably improved Li behavior properties of the G+MG/Cu (i.e., high specific capacity retention and excellent rate cycling performance) may be attributed to the electrochemically and mechanically enhanced interfacial properties of active materials via graphene nanosheets.

## CONCLUSIONS

In summary, we have proposed and developed a novel concept of interface engineering between the active material and the current collector in LIBs that a graphene interfacial layer grown directly on Cu current collectors offers multiple synergistic effects to the electrochemical behavior and structural stability of electrode materials. We have demonstrated that the MG/Cu exhibits the remarkably improved electrochemical performance with high reversible capacity, excellent rate-performance, and cycling stability over 100 cycles compared to the bare Cu. These excellent electrochemical features can be explained by the unique multifunctional effects of graphene interlayers on the structural stability, charge transfer kinetics, and Cu oxidation or corrosion reaction as well as interfacial adhesion. Moreover, we have further optimized the interface of active materials with graphene in order to enhance the overall electrochemical performance of cells, exhibiting the high reversible capacity of 708 mAh $g^{-1}$. Our findings suggest that the interface engineering based on graphene might be an attractive potential strategy not only for fundamental studies related to interfacial phenomena in electrochemical conversion


DOI: 10.1021/acsami.6b03866
ACS Appl. Mater. Interfaces 2016, 8, 17651−17658

and storage systems but also for practical uses in various viable electronic and energy devices.

## ■ ASSOCIATED CONTENT

### Supporting Information

The Supporting Information is available free of charge on the ACS Publications website at DOI: 10.1021/acsami.6b03866.

Photograph image and XPS spectra of the graphene directly grown on Cu foil; electrochemical performance and cross-sectional SEM analysis of the electrodes; summarized tables for electrochemical behavior properties of all electrodes (PDF)

## ■ AUTHOR INFORMATION


### Corresponding Authors

*E-mail hjahn@seoultech.ac.kr (H.-J.A.).
*E-mail junginn.sohn@eng.ox.ac.uk (J.I.S.).

### Author Contributions

Y.-W.L. and G.-H.A. contributed equally to this work.


### Notes

The authors declare no competing financial interest.

## ■ ACKNOWLEDGMENTS

This research was supported by the International Collaborative Energy Technology R&D Program of the Korea Institute of Energy Technology Evaluation and Planning (KETEP, No. 20138520030800), and the Industrial Fundamental Technology Development Program (10052745, Development of nanosized (100 nm) manganese ceramic material for high voltage pseudocapacitor) funded by the Ministry of Trade, Industry and Energy (MOTIE) of Korea.

## ■ REFERENCES


(1) Tarascon, J.-M.; Armand, M. Issues and Challenges Facing Rechargeable Lithium Batteries. *Nature* **2001**, *414*, 359−367.

(2) Graetzel, M.; Janssen, R. A. J.; Mitzi, D. B.; Sargent, E. H. Materials Interface Engineering for Solution-Processed Photovoltaics. *Nature* **2012**, *488*, 304−312.

(3) Di, C.-A.; Liu, Y.; Yu, G.; Zhu, D. Interface Engineering: An Effective Approach toward High-Performance Organic Field-Effect Transistors. *Acc. Chem. Res.* **2009**, *42*, 1573−1583.

(4) Wang, L.; Wang, D.; Dong, Z.; Zhang, F.; Jin, J. Interface Chemistry Engineering for Stable Cycling of Reduced GO/$SnO_2$ Nanocomposites for Lithium Ion Battery. *Nano Lett.* **2013**, *13*, 1711−1716.

(5) Lahiri, I.; Oh, S.-W.; Hwang, J. Y.; Cho, S.; Sun, Y.-K.; Banerjee, R.; Choi, W. High Capacity and Excellent Stability of Lithium Ion Battery Anode Using Interface-Controlled Binder-Free Multiwall Carbon Nanotubes Grown on Copper. *ACS Nano* **2010**, *4*, 3440−3446.

(6) Kim, M.-C.; Lee, Y.-W.; Kim, S.-J.; Hwang, B.-M.; Park, H.-C.; Hwang, E.-T.; Cao, G.; Park, K.-W. Improved Lithium Ion Behavior Properties of $TiO_2$@Graphitic-like Carbon Core@Shell Nanostructure. *Electrochim. Acta* **2014**, *147*, 241−249.

(7) Wang, D.; Yu, Y.; He, H.; Wang, J.; Zhou, W.; Abruña, H. D. Template-Free Synthesis of Hollow-Structured $Co_3O_4$ Nanopartiles as High-Performance Anodes for Lithium Ion Batteries. *ACS Nano* **2015**, *9*, 1775−1781.

(8) Wan, X.; Chen, K.; Xu, J. Interface Engineering for CVD Graphene: Current Status and Progress. *Small* **2014**, *10*, 4443−4454.

(9) Yu, G.; Hu, L.; Vosgueritchian, M.; Wang, H.; Xie, X.; McDonough, J. R.; Cui, X.; Cui, Y.; Bao, Z. Solution-Processed Graphene/$MnO_2$ Nanostructured Textiles for High-Performance Electrochemical Capacitors. *Nano Lett.* **2011**, *11*, 2905−2911.

(10) Huang, X.-I.; Wang, R.-Z.; Wang, Z.-I.; Wang, H.-G.; Xu, J.-J.; Wu, Zn.; Liu, Q.-C.; Zhang, Y.; Zhang, X.-B. Homogeneous CoO on Graphene for Binder-Free and Ultralong-Life Lithium Ion Batteries. *Adv. Funct. Mater.* **2013**, *23*, 4345−4353.

(11) Wang, R.; Xu, C.; Sun, J.; Gao, L.; Lin, C. Flexible Free-Standing Hollow $Fe_3O_4$/Graphene Hybrid Films for Lithium-Ion Batteries. *J. Mater. Chem. A* **2013**, *1*, 1794−1800.

(12) Wang, K.-X.; Li, X.-H.; Chen, J.-S. Surface and Interface Engineering of Electrode Materials for Lithium Ion Batteries. *Adv. Mater.* **2015**, *27*, 527−545.

(13) Kim, M.-C.; Lee, Y.-W.; Kim, S.-J.; Kwak, D.-H.; Park, H.-C.; Kim, D.-M.; Park, K.-W. High Volumetric Energy Density Lithium Ion Battery with Titania@Carbon Nanostructure Electrode. *Int. J. Electrochem. Sci.* **2015**, *10*, 8993−9005.

(14) Oh, M. H.; Yu, T.; Yu, S.-H.; Lim, B.; Ko, K.-T.; Willinger, M.-G.; Seo, D.-H.; Kim, B. H.; Cho, M. G.; Park, J.-H.; Kang, K.; Sung, Y.-E.; Pinna, N.; Hyeon, T. Galvanic Replacement Reactions in Metal Oxide Nanocrystals. *Science* **2013**, *340*, 964−968.

(15) Hwang, J.; Jo, C.; Kim; Kim, M. G.; Chun, J.; Lim, E.; Kim, S.; Jeong, S.; Kim, Y.; Lee, J. Mesoporous Ge/$GeO_2$/Carbon Lithium-Ion Battery Anodes with High Capacity and High Reversibility. *ACS Nano* **2015**, *9*, 5299−5309.

(16) Yu, L.; Qian, Z.; Shi, N.; Liu, Q.; Wang, J.; Jing, X. Interface Chemistry Engineering in Electrode Systems for Electrochemical Energy Storage. *RSC Adv.* **2014**, *4*, 37491−37502.

(17) Du, F.-H.; Wang, K.-X.; Chen, J.-S. Strategies to Succeed in Improving the Lithium-Ion Storage Properties of Silicon Nanomaterials. *J. Mater. Chem. A* **2016**, *4*, 32−50.

(18) Rozada, R.; Paredes, J. I.; López, M. J.; Villar-Rodil, S.; Cabria, I.; Alonso, J. A.; Martínez-Alonso, A.; Tascón, J. M. D. From Graphene Oxide to Pristine Graphene: Revealing the Inner Workings of the Full Structural Restoration. *Nanoscale* **2015**, *7*, 2374−2390.

(19) Paredes, J. I.; Villar-Rodil, S.; Solís-Fernandez, P.; Martínez-Alonso, A.; Tascón, J. M. D. Atomic Force and Scanning Tunneling Microscopy Imaging of Graphene Nanosheets Derived from Graphite Oxide. *Langmuir* **2009**, *25*, 5957−5968.

(20) Xu, K.; Cao, P.; Heath, J. R. Graphene Visualizes the First Water Adlayers on Mica at Ambient Conditions. *Science* **2010**, *329*, 1188−1191.

(21) Sun, Z.; Yan, Z.; Yao, J.; Beitler, E.; Zhu, Y.; Tour, J. M. Growth of Graphene from Solid Carbon Sources. *Nature* **2010**, *468*, 549−552.

(22) Liu, Y.; Liu, Z.; Lew, W. S.; Wang, Q. J. Temperature Dependene of the Elecctrical Transport Properties in Few-Layer Graphene Interconnects. *Nanoscale Res. Lett.* **2013**, *8*, 335.

(23) Zhu, S.-E.; Yuan, S.; Janssen, G. C. A. M. Optical Transmittance of Multilayer Graphene. *EPL* **2014**, *108*, 17007.

(24) Wu, L.; Chu, H. S.; Koh, W. H.; Li, E. P. Highly Sensitive Graphene Biosensors based on Surface Plasmon Resonance. *Opt. Express* **2010**, *18*, 14395−14400.

(25) Nair, R. R.; Blake, P.; Grigorenko, A. N.; Novoselov, K. S.; Booth, T. J.; Stauber, T.; Peres, N. M. R.; Geim, A. K. Fine Structure Constant Defines Visual Transparency of Graphene. *Science* **2008**, *320*, 1308.

(26) Gao, X.; Luo, W.; Zhong, C.; Wexler, D.; Chou, S.-L.; Liu, H.-K.; Shi, Z.; Chen, G.; Ozawa, K.; Wang, J.-Z. Novel Germanium/Polypyrrole Composite for High Power Lithium-Ion Batteries. *Sci. Rep.* **2014**, *4*, 6095.

(27) Osaka, T.; Nara, H.; Momma, T.; Yokoshima, T. New S-O-C Composite Film Anode Materials for LIB by Electrodeposition. *J. Mater. Chem. A* **2014**, *2*, 883−896.

(28) Liu, H.-C.; Yen, S.-K. Characterization of Electrolytic $Co_3O_4$ Thin Films as Anode for Lithium-Ion Batteries. *J. Power Sources* **2007**, *166*, 478−484.

(29) Li, B.; Cao, H.; Shao, J.; Li, G.; Qu, M.; Yin, G. $Co_3O_4$@graphene Composites as Anode Materials for High-Performance Lithium Ion Batteries. *Inorg. Chem.* **2011**, *50*, 1628−1632.

(30) Ye, J.; An, Y.; Montalvo, E.; Campbell, P. G.; Worsley, M. A.; Tran, I. C.; Liu, Y.; Wood, B. C.; Biener, J.; Jiang, H.; Tang, M.; Wang, Y. M. Solvent-Directed Sol-Gel Assembly of 3-Dimensional Graphene-




DOI: 10.1021/acsami.6b03866
*ACS Appl. Mater. Interfaces* 2016, 8, 17651−17658

Tented Metal Oxides and Strong Synergistic Disparities in Lithium Storage. *J. Mater. Chem. A* **2016**, *4*, 4032−4043.
(31) Wu, Z.-S.; Ren, W.; Wen, L.; Gao, L.; Zhao, J.; Chen, Z.; Zhou, G.; Li, F.; Cheng, H.-M. Graphene Anchored with Co3O4 Nanoparticles as Anode of Lithium Ion Batteries with Enhanced Reversible Capacity and Cyclic Performance. *ACS Nano* **2010**, *4*, 3187−3194.
(32) Yu, M.; Wang, W.; Li, C.; Zhai, T.; Lu, X.; Tong, Y. Scalable Self-Growth of Ni@NiO Core-Shell Electrode with Ultrahigh Capacitanccce and Super-Long Cyclic Stability for Supercapacitors. *NPG Asia Mater.* **2014**, *6*, e129.
(33) Oumellal, Y.; Delpuech, N.; Mazouzi, D.; Dupré, N.; Gaubicher, J.; Moreau, P.; Soudan, P.; Lestriez, B.; Guyomard, D. The Failure Mechanism of Nano-Sized Si-based Negative Electrodes for Lithium Ion Batteries. *J. Mater. Chem.* **2011**, *21*, 6201−6208.
(34) Hou, J.; Cao, C.; Ma, X.; Idrees, F.; Xu, B.; Hao, X.; Lin, W. From Rice Bran to High Energy Density Supercapacitors: A New Route to Control Porous Structure of 3D Carbon. *Sci. Rep.* **2014**, *4*, 7260.
(35) Sakunthala, A.; Reddy, M. V.; Selvasekarapandian, S.; Chowdari, B. V. R.; Selvin, P. C. Energy Storage Studies of Bare and Doped Vanadium Pentoxide, $(V_{1.95}M_{0.05})O_5$, M = Nb, Ta, for Lithium Ion Batteries. *Energy Environ. Sci.* **2011**, *4*, 1712−1725.
(36) Jana, S. K.; Saha, B.; Satpati, B.; Banerjee, S. Structural and Electrochemical Analysis of a Novel Co-Electrodeposited $Mn_2O_3$-Au Nanocomposite Thin Film. *Dalton Trans.* **2015**, *44*, 9158−9169.
(37) Sultana, I.; Rahman, M. M.; Ramireddy, T.; Sharma, N.; Poddar, D.; Khalid, A.; Zhang, H.; Chen, Y.; Glushenkov, A. M. Understanding Structure-Function Relationship in Hybrid $Co_3O_4$-$Fe_2O_3$/C Lithium-Ion Battery Electrodes. *ACS Appl. Mater. Interfaces* **2015**, *7*, 20736−20744.
(38) Ming, H.; Ming, J.; Oh, S.-M.; Tian, S.; Zhou, Q.; Huang, H.; Sun, Y.-K.; Zheng, J. Surface-Assisted Synthesis of $Fe_2O_3$ Nanoparticles and F-Doped Carbon Modification toward an Improved $Fe_3O_4$@$CF_x$/$LiNi_{0.5}Mn_{1.5}O_4$ Battery. *ACS Appl. Mater. Interfaces* **2014**, *6*, 15499−15509.
(39) Moulder, J. F.; Stickle, W. F.; Sobol, P. E.; Bomben, K. D. *Handbook of X-ray Photoelectron Spectroscopy*; Physical Electronics, Inc.: 1995.
(40) Mondal, P.; Sinha, A.; Salam, N.; Roy, A. S.; Jana, N. R.; Islam, S. M. Enhanced Catalytic Performance by Copper Nanoparticle-Graphene based Composite. *RSC Adv.* **2013**, *3*, 5615−5623.


DOI: 10.1021/acsami.6b03866
*ACS Appl. Mater. Interfaces* 2016, 8, 17651−17658